Nanotechnology **22** (2011) 295710 (7pp) doi:10.1088/0957-4484/22/29/295710

'Sub-atomic' resolution of non-contact atomic force microscope images induced by a heterogeneous tip structure: a density functional theory study

Anna Campbellová[1], Martin Ondráček[2], Pablo Pou[3], Rubén Pérez[3], Petr Klapetek[1] and Pavel Jelínek[2]

[1] Czech Metrology Institute, Okružní 31, 638 00, Brno, Czech Republic
[2] Institute of Physics, Academy of Sciences of the Czech Republic, Cukrovarnická 10, 162 00 Prague, Czech Republic
[3] Departamento de Física Teórica de la Materia Condensada, Universidad Autónoma de Madrid, 28049 Madrid, Spain

E-mail: jelinekp@fzu.cz

Received 4 March 2011, in final form 25 May 2011
Published 20 June 2011
Online at stacks.iop.org/Nano/22/295710

Abstract

A Si adatom on a Si(111)-(7 × 7) reconstructed surface is a typical atomic feature that can rather easily be imaged by a non-contact atomic force microscope (nc-AFM) and can be thus used to test the atomic resolution of the microscope. Based on our first principles density functional theory (DFT) calculations, we demonstrate that the structure of the termination of the AFM tip plays a decisive role in determining the appearance of the adatom image. We show how the AFM image changes depending on the tip–surface distance and the composition of the atomic apex at the end of the tip. We also demonstrate that contaminated tips may give rise to image patterns displaying so-called 'sub-atomic' features even in the attractive force regime.

(Some figures in this article are in colour only in the electronic version)

1. Introduction

The analysis, control and modification of molecules, surfaces or nanostructures are nowadays among the greatest challenges to the emerging field of nanotechnology. Nanoprobe techniques such as the scanning tunnelling microscope (STM) [1] and the atomic force microscope (AFM) [2] accomplish these goals. During the last 15 years, frequency modulation (FM) AFM [3–5] has experienced especially fast development. This technique has already revealed many outstanding capabilities in ultrahigh vacuum (UHV) conditions including atomic scale imaging (see e.g. [6–10]) and manipulation, e.g. [11–15] on metallic, semiconductor or insulator surfaces. Even sub-atomic resolution on some surfaces has been reported [16–18]. High-precision measurements of the short-range chemical forces have become possible with dynamic force spectroscopy (DFS) [19, 10]. Furthermore, chemical discrimination of individual atoms based on chemical force analysis has also been achieved [20]. DFS even allows the mapping of three-dimensional force fields with atomic resolution [13, 21–24]. In principle, these measurements could provide, by an elaborate separation of the short-range contribution from the total force, detailed information about surface energy landscapes, adhesion forces and the spatial resolution of the inter-atomic forces.

Further development of the FM-AFM technique depends on a detailed understanding of the mechanisms of interaction between the AFM tip and the sample at the atomic scale. This knowledge would help to optimize scanning conditions for imaging and manipulation of individual atoms and also to exclude any of the artefacts which so often appear in scanning probe microscopy (SPM) techniques [25]. Many theoretical works explaining the origin of the atomic contrast on different surfaces have already been published [8, 9, 26–30]. However, a reliable interpretation of the energy landscapes and the atomic topography of the surface provided by recent 3D

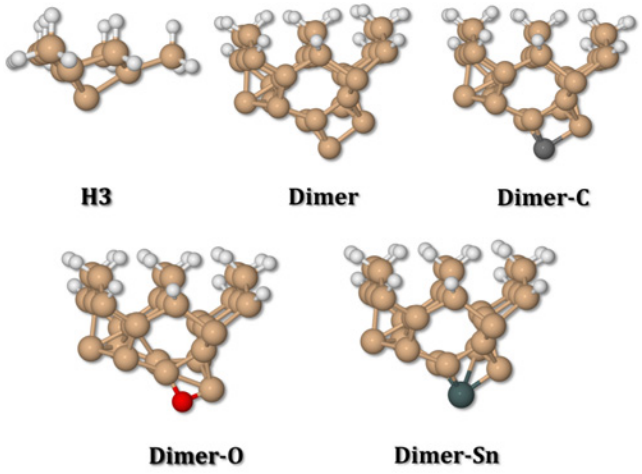

Figure 1. Ball and stick models of the Si-based clusters used in our simulations to mimic AFM tips. The H3 tip is based on the H_3-like configuration of the Si(111) surface. The dimer tip, which is based on a cluster grown in the (001) direction, is characterized by Si dimer termination. In the dimer-C, -O and -Sn tips the outermost Si atom of the dimer-like tip is respectively substituted by a carbon, oxygen or tin atom.

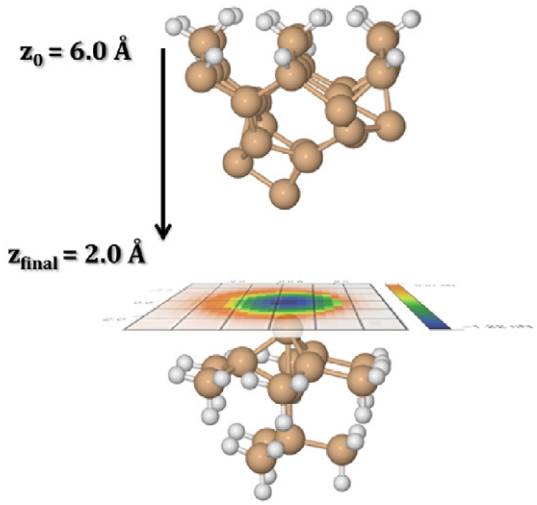

Figure 2. Ball and stick model of the simulated system; the Si dimer tip is placed over the cluster that mimics a Si adatom of the Si(111)-(7 × 7) surface. Force versus distance curves are calculated on a 25 × 25x–y grid.

experimental mappings [13, 21–24] requires a more complete theoretical study, taking explicitly into account the chemical composition of the probe. In this paper we provide a detailed analysis of the influence of the atomic tip structure on the 3D spatial resolution of a single atom using density functional theory (DFT) simulations. In particular, we have performed DFT simulations of a 3D scan over a silicon cluster, which reproduces the local coordination of a surface adatom, using different pristine or contaminated Si-based tips [28]. The aim of this work is to reveal the effect of the atomic termination of the apex on the atomic scale AFM images of semiconductor surfaces.

We focus on the Si(111)-(7 × 7) surface that is perhaps the most studied semiconductor surface. On this surface, many interesting phenomena have been reported, including sub-atomic patterns on Si adatoms [16]. Despite considerable theoretical efforts [31, 32], the origin of these sub-atomic features is still under debate and not completely understood [33].

2. Methods

Our calculations, performed with the FIREBALL code [34, 35], are based on DFT [36] with a local-orbital basis. This code offers a very favourable accuracy-to-efficiency balance as long as the basis set is carefully chosen [37]. In this particular case, our numerical basis set had the following cutoff radii (in au) of the orbitals: 3.8 (s) for H, 3.3 (s and s*), 3.8 (p and p*) for O orbitals and (4.5, 4.5), (4.8, 5.4) and (5.2, 5.7) for the (s, p) orbitals of C, Si and Sn, respectively. The calculations were performed as non-spin-polarized and within the local-density approximation (LDA) for the exchange–correlation functional [36, 38].

AFM probes were simulated by a set of mechanically stable [28, 39] and well-tested Si(111) nanoasperities of Si atoms that closely reproduce the experimental short-range force curves measured over a Si adatom [20]. In addition, as oxygen and carbon atoms are likely to be present in a UHV chamber during experiments, we extended our tip set by similar models including contaminants at the apex position, such as Sn, C and O. All tip models and the corresponding nomenclature are shown in figure 1. Only H atoms and the topmost Si layer were fixed in the tip models, the other atoms were allowed to assume their equilibrium positions. It would be too demanding to carry out complete calculations of 3D mapping over a Si adatom on the Si(111)-(7 × 7) surface within the DFT accuracy, while we also need to consider several different tip models (see figure 1). Therefore we adopted a simplified atomistic model that mimics the surface well. It consisted of a small cluster of 15 Si atoms arranged in the same relative atomic positions as those of a Si adatom and its 14 nearest neighbours on the Si(111)-(7 × 7) surface. These 14 Si neighbours were passivated by 27 H atoms (see figure 2). During the optimization process, only the five central Si atoms were allowed to relax. To check the validity of our cluster approximation, we performed vertical scans with two different tips on the Si corner adatom of the Si(111)-(7 × 7) surface in both the cluster model and in a slab model (see figure 3). The surface in the slab was modelled by seven Si layers and an additional H passivating layer, 347 atoms in total. We let the six top Si layers of the slab relax, while the rest of the atoms were kept fixed during the optimization process. The calculations were carried out with only the Γ point for the sampling of the Brillouin zone. The geometry was converged until the criteria of 10^{-6} eV and 0.05 eV $Å^{-1}$ for the accuracy in energy and force were respectively satisfied. We mapped the tip–sample interaction for different values of the tip–sample distance, subsequently approaching the tip towards the surface in a quasi-static manner: starting at an initial tip–sample distance we optimized the atomic positions, then we shifted the tip atoms by 0.25 Å downward and repeated the optimization

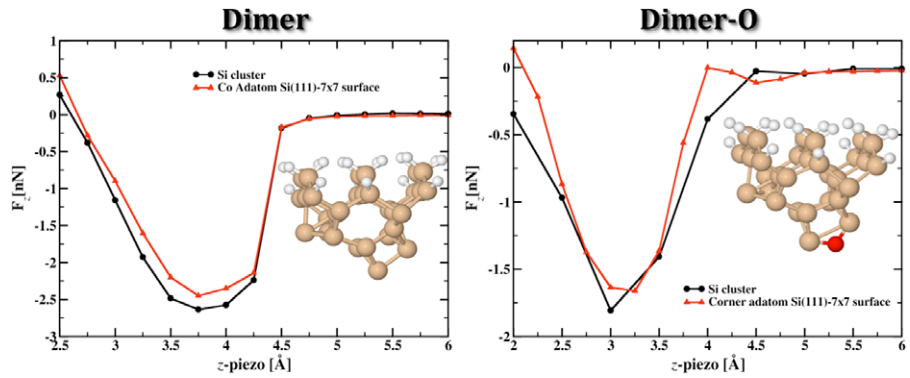

Figure 3. Comparison of the calculated short-range force for the clean Si dimer tip (left) and the O-contaminated dimer-O tip (right) acting on a Si adatom in the slab Si(111)-(7 × 7) and the Si cluster model.

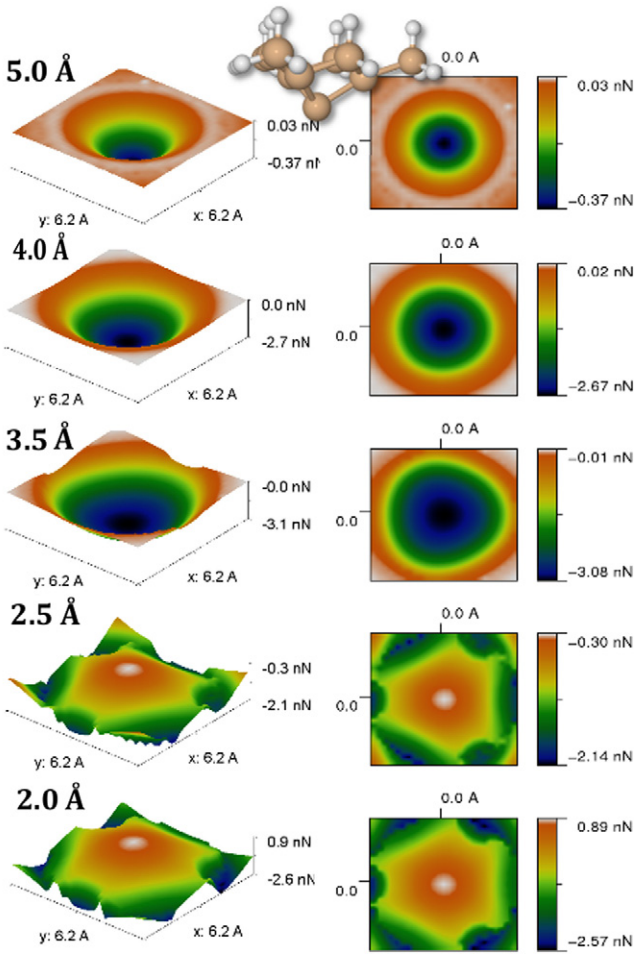

Figure 4. Forces between the H3-type Si apex and the adatom-like cluster shown as 2D colour maps at different tip–cluster distances. At the larger distances the image shows a circular shape. Upon approaching the tip towards the cluster, the image evolves to a slightly asymmetric pattern with a triangular shape; the effect becomes drastic at the shorter distances where the repulsive interaction starts to act.

process for the new tip position. Optionally, we applied a shift of 0.1 Å in areas of interest where the atomic scale contrast changes rapidly (see figure 6). In order to simulate a 3D map, we carried out a set of vertical scans on a rectangular xy-mesh of 25 × 25 points, covering a 6 × 6 Å^2 square area and centred around the Si adatom (see figure 4).

3. Results

3.1. Force site spectroscopy

Dynamic force spectroscopy [19, 20, 40] can provide valuable information about the chemical force acting between the outermost atoms of the tip and the sample. Direct comparison between the available experimental short-range forces and theoretical curves opens up a way to characterize the atomic and chemical structure of the tip. Figure 3 shows force versus distance curves obtained over a Si adatom on the Si(111)-(7 × 7) surface using different tips, in particular the dimer-terminated clean Si probe (dimer) and the O-contaminated Si probe (dimer-O). We can immediately see that not only the maximal attractive force but also a decay of the attractive chemical force changes significantly. Later on, we will also analyse a modification of the spatial resolution with tip termination at various tip–sample distances.

As mentioned in section 2, we have verified the validity of the cluster approximation, which we use to describe the reconstructed Si surface, by performing selected vertical scans in both the cluster and the slab model. We have found very good agreement between the two models, as shown in figure 3. In the case of a bare Si tip both curves are almost identical. A small difference arises only in the region of the strongest interaction, where the mechanical response of the whole surface is more important. In the case of an oxygen-contaminated tip, we see a slight difference between the two models at the onset of the chemical force. This difference comes mainly from the presence of the long-range electrostatic force induced by a charge transfer between the apex oxygen atom and the surrounding silicon atoms of the tip. Still, these small discrepancies do not affect the lateral resolution on a Si adatom discussed in this paper.

3.2. 3D mapping

Si adatoms on the Si(111)-(7 × 7) surface are usually imaged as spherical entities. This picture is endorsed by our theoretical

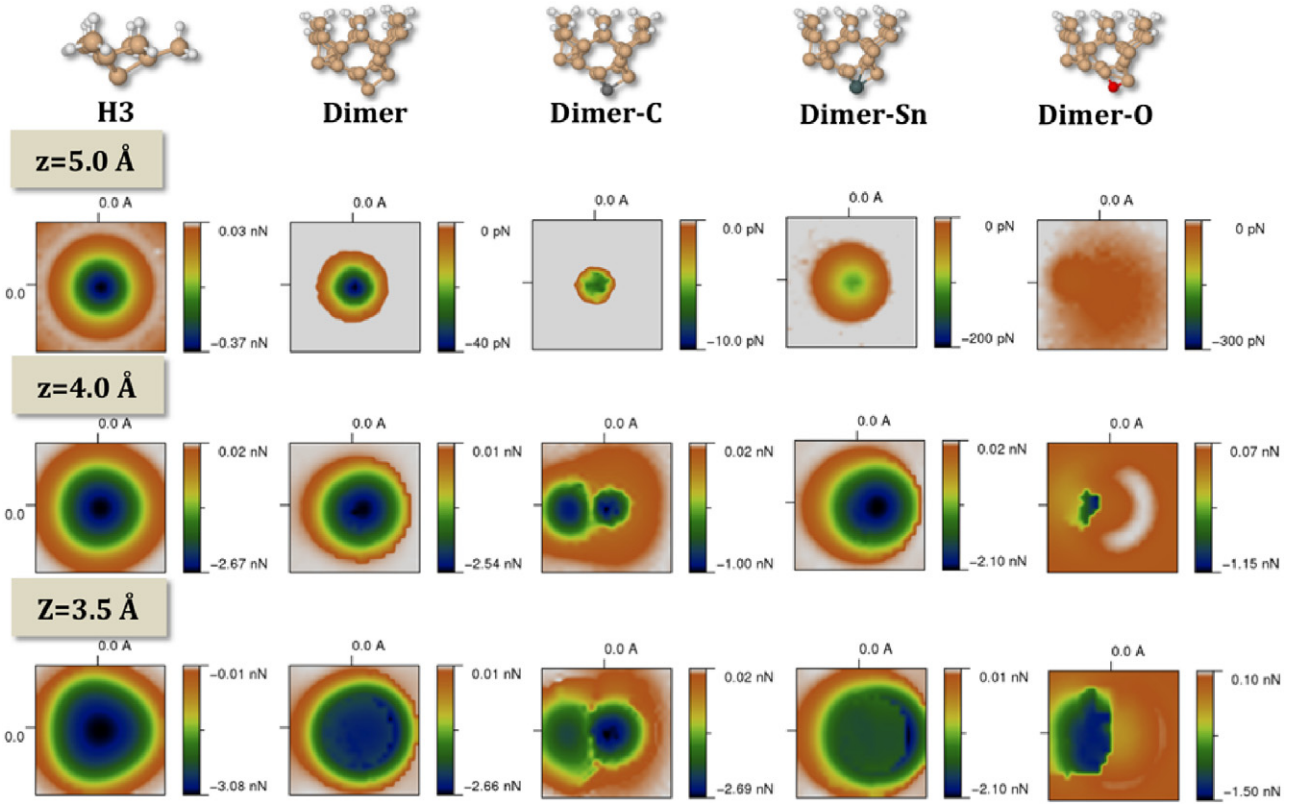

Figure 5. 2D force colour maps for the tip models simulated in this work for three (5, 4 and 3.5 Å) tip–cluster distances. Circular patterns, only slightly distorted, are found for the pure Si apexes and also for the Sn-contaminated tip (H3, dimer and dimer-Sn tips). However, when the chemical species of the contaminant has a different reactivity or interaction range, in this study for the O- or C-contaminated tips (dimer-O and dimer-C), the image is clearly asymmetric, displaying even in the attractive regime two protrusions that originate from the dimer structure of the apex.

simulation using the H3 model of a clean Si probe (see figure 4). This tip model is made up by a (111) orientation cluster with an apex Si atom sitting in the H_3 position [28] with a characteristic half-filled localized dangling bond state. We can see how the spherical shape observed in the attractive regime gradually changes to a three-fold symmetry pattern when the repulsive regime over the adatom is reached. This three-fold pattern in the close distance regime is caused by an interplay between the repulsive interaction on the adatom and the attractive interaction acting between the apex tip atom and the three silicon atoms in the next surface layer.

In the next step, we performed similar calculations using other tip models, based on the Si(100) surface face, on which the apex is formed by a dimer-like heterostructure resembling the Si(100)-p(2 × 1) reconstruction and may include different contaminants such as O, C and Sn. The variation of the atomic pattern with a decrease in the tip–sample distance in the attractive regime is shown in figure 5. In the far distance regime, over ≈5.0 Å, the spherical atomic pattern is observed independently of the tip model, apart from the dimer-O with an oxygen impurity atom in the apex position for which the short-range forces are negligible (see figure 3). In the case of the pure silicon dimer model and the dimer-Sn model with a tin atom in the apex position, we have found only slight asymmetric distortions from the spherical shape observed with the clean H3 model. However, the presence of an alien carbon or oxygen atom in the apex position produces drastic changes in the pattern symmetry, reflecting the heterodimer structure of the tip apex. This asymmetry comes mainly from the influence of the neighbouring Si atom forming the dimer, which also starts to interact with the adatom below a certain distance. This effect is much smaller in the case of the dimer and dimer-Sn models because of the larger interaction range of the Si or Sn outermost apex atoms (compared to the C or O atoms), which screens the influence of the other dimer atom in the attractive regime. In the case of the dimer-O model, the main attractive force comes just from the second Si dimer atom. This attractive force produces a vertical flip of the dimer at closer distances: the Si dimer atom moves closer to the surface while the oxygen atom retracts away from the surface. The asymmetry induced by the dimer-derived contaminated tips will obviously lead to the dependence of the resulting image on the orientation of the scanning probe with respect to the imaged surface. However, our results show that the effect of the asymmetry becomes sizeable only when the tip scans close to the surface, in the regime of a strong attractive force.

Let us note that in our calculations we have found the heterodimer models to be mechanically stable (the same tip structure is recovered after an approach–retraction cycle) even when subjected to substantial pressure in the repulsive regime with a maximal force of ≈0.5 nN. However, in the repulsive regime, dimer-like models suffer significant

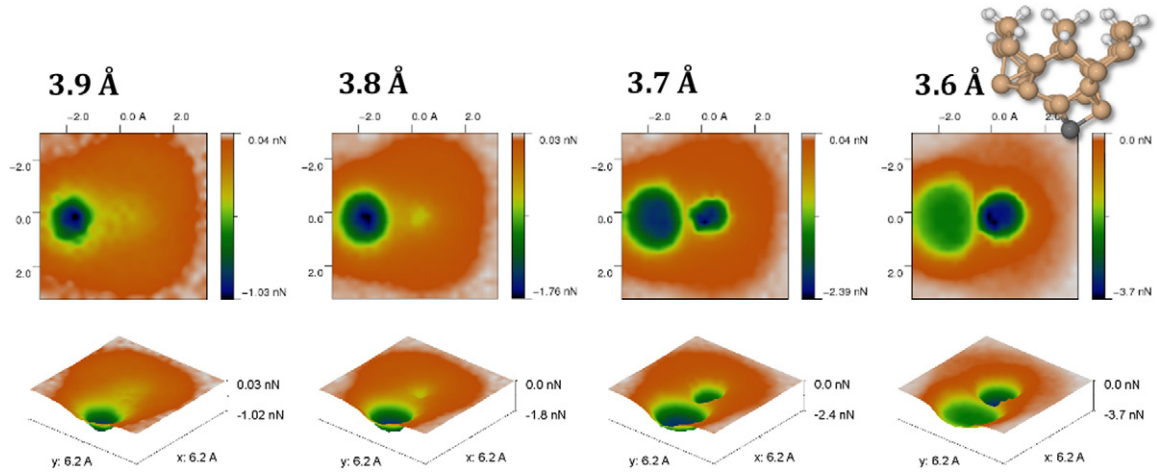

Figure 6. 2D force maps for the C-terminated (dimer-C) tip in the distance range from 3.9 Å down to 3.6 Å where the image asymmetry becomes apparent and resembles a 'sub-atomic' feature.

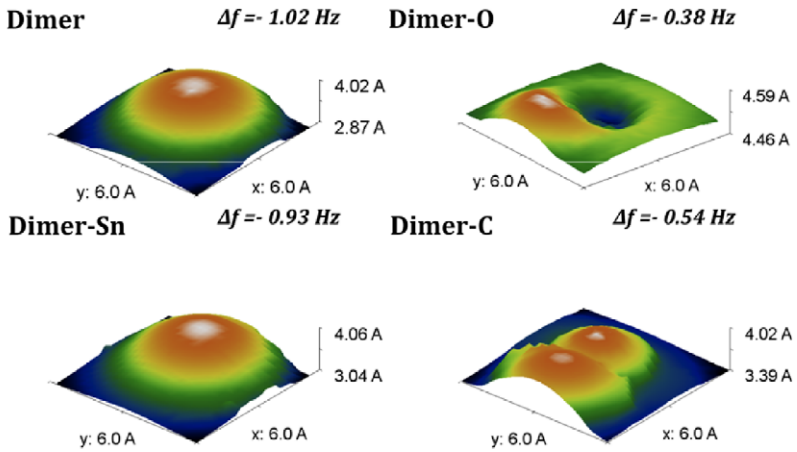

Figure 7. Simulated constant frequency images for the dimer-like Si tip models in the attractive interaction regime. Atomic contrast strongly varies with the chemical structure of the outermost atoms.

reversible deformations, mainly of the apex part, making the atomic pattern even more irregular. Keeping in mind that the cluster approximation is not well justified in the repulsive regime, we do not further discuss the atomic patterns obtained at this distance range here.

A detailed look into the atomic image produced by the carbon-contaminated (dimer-C) probe model in a distance range of ≈3.9–3.6 Å (see figure 6) reveals a pattern similar to the so-called sub-atomic features observed on the Si(111)-(7 × 7) surface by AFM [16]. Indeed, the image shows two crescents with a spherical envelope separated by ≈2 Å, close to the experimental observation [16]. In our simulations, the origin of these two crescents is clearly due to the interaction of both C and Si dimer atoms with the Si adatom depending on the lateral position of the tip with respect to the surface adatom. In previous works [16, 31, 32] this type of image was attributed to two atomic orbitals of the front silicon atom, which had only two bonds to the silicon atoms underneath the tip. However, this kind of atomic configuration is unlikely due to the presence of the two unsaturated bonds and it easily undergoes transition to a more stable configuration [28]. Indeed, both previous theoretical works [31, 32] did not take into account the atomic relaxation of the tip structure due to the interaction with the sample.

We should note that the original experimental image was acquired in the constant frequency shift regime. In order to make a direct comparison with the original image, we calculated the frequency shift from our force versus distance data using appropriate integral formulae [4] and extracted the tip–sample distance 2D-map corresponding to a constant frequency shift. In order to make the comparison with experiment more straightforward, a long-range force was added to the calculated short-range force. The long-range force F_{LR} was estimated using the analytical model [41] $F_{\mathrm{LR}} = -\frac{A_{\mathrm{H}}R}{6(z+z_o)^2}$, where A_{H} is the Hamaker constant, R the tip radius, z is the tip–sample distance and z_o is a constant. Here, we used the values $A_{\mathrm{H}}R = 175$ nN Å^2 and $z_o = 1.28$ Å frequently observed in experimental measurements with Si-cantilevers [42]. The constant frequency images constructed in this way are shown in figure 7. The frequency shift set point was chosen so that it resulted in typical attractive-regime images, corresponding to a tip height of $z = 4.0$ Å on top of the

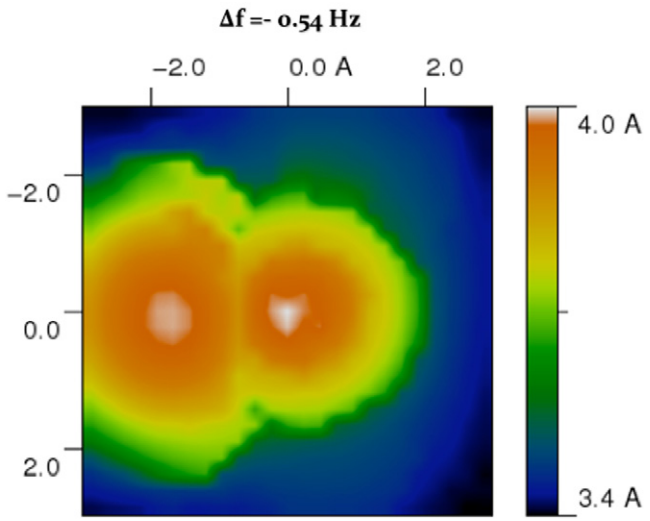

Figure 8. Detailed view of the simulated constant Δf image of a Si adatom obtained with the carbon-contaminated (i.e. dimer-C) tip. The image shows a double protrusion pattern similar to the 'sub-atomic' feature reported in [16].

adatom, except for the dimer-O case, for which the tip height on the adatom was set to $z = 4.5$ Å. The resulting pictures keep the same characteristics as the original constant height maps of forces in figure 5. In particular, the picture obtained with the C-contaminated tip shows the two protrusions separated by ≈2 Å with a corrugation height of ≈0.6 Å. A close-up view of the constant frequency image for this tip is also shown in figure 8.

4. Conclusions

A detailed analysis of the atomic patterns of an individual Si adatom with several pristine or contaminated Si-based tips has been performed using DFT simulations. We have found a strong variation of the internal atomic pattern with the symmetry and chemical composition of the tip apex. The theoretical atomic image provided by a dimer-like Si tip with a carbon atom positioned on the apex has similar characteristics to the sub-atomic features observed in experiment [16]. Therefore, our calculations indicate an alternative origin of the sub-atomic pattern observed on the Si adatom, namely a contaminated probe.

Based on the presented theoretical analysis, it is evident that the atomic scale AFM images taken near the contact regime incorporate the structure of both the sample and the outermost apex atoms. This convolution process is especially prominent if atoms of different chemical species are present on the tip apex. This effect should be particularly considered during the analysis of 3D spectroscopy measurements, where the tip structure can greatly spoil the potential energy surfaces derived from the experimental data.

Acknowledgments

We are grateful to Dr Y Sugimoto and Professors S Morita and F J Giessibl and Dr O Custance for inspiring discussions. PJ and MO have been supported in this work by the GAAV grants nos M100100904 and IAA100100905 and the GAČR project no. 204/10/0952. MO acknowledges the support provided by the Czech Science Foundation (GAČR) under the postdoctoral project P204/11/P578. AC and PK gratefully acknowledge the support of the Grant Agency of the Academy of Sciences of the Czech Republic (GAAV) under contract KAN311610701. PP acknowledges the support of the Ramón y Cajal Programme (MICINN, Spain). PP and RP are supported by projects MAT2008-02929-NAN, MAT2008-02939-E, CSD2010-00024 (MICINN, Spain) and S2009/MAT-1467 (Comunidad Autónoma de Madrid, Spain).

References

[1] Binning G, Rohrer H, Gerber Ch and Weibel E 1982 *Phys. Rev. Lett.* **49** 57–61
[2] Binning G, Quate C F and Gerber Ch 1986 *Phys. Rev. Lett.* **56** 930–3
[3] García R and Pérez R 2002 *Surf. Sci. Rep.* **47** 197–301
[4] Giessibl F J 2003 *Rev. Mod. Phys.* **75** 949–83
[5] Morita S, Giessibl F J and Wiesendanger R (ed) 2009 *Noncontact Atomic Force Microscopy* (*NanoScience and Technology* vol 2) ed Avouris *et al* (Berlin: Springer)
[6] Giessibl F J 1995 *Science* **267** 68–71
[7] Barth C and Reichling M 2001 *Nature* **414** 54–7
[8] Foster A S, Barth C, Shluger A L and Reichling M 2001 *Phys. Rev. Lett.* **86** 2373–6
[9] Bechstein R, González C, Schütte J, Jelínek P, Pérez R and Kühnle A 2009 *Nanotechnology* **20** 505703
[10] Gross L, Mohn F, Moll N, Liljeroth P and Meyer G 2009 *Science* **325** 1110–4
[11] Sugimoto Y *et al* 2005 *Nat. Mater.* **4** 156–9
[12] Sugimoto Y *et al* 2007 *Phys. Rev. Lett.* **98** 106104
[13] Ternes M, Lutz Ch P, Hirjibehedin C F, Giessibl F J and Heinrich A J 2008 *Science* **319** 1066–9
[14] Sugimoto Y *et al* 2008 *Science* **322** 413–7
[15] Hirth S, Ostendorf F and Reichling M 2006 *Nanotechnology* **17** S148–54
[16] Giessibl F J, Hembacher S, Bielefeldt H and Mannhart J 2000 *Science* **289** 422–5
[17] Herz M, Giessibl F J and Mannhart J 2003 *Phys. Rev.* B **68** 045301
[18] Hembacher S, Giessibl F J and Mannhart J 2004 *Science* **305** 380–3
[19] Lantz M A, Hug H J, Hoffmann R, van Schendel P J A, Kappenberger P, Martin S, Baratoff A and Güntherodt H J 2001 *Science* **291** 2580–3
[20] Sugimoto Y *et al* 2007 *Nature* **446** 64–7
[21] Hölscher H, Langkat S M, Schwarz A and Wiesendanger R 2002 *Appl. Phys. Lett.* **81** 4428–30
[22] Albers B J *et al* 2009 *Nat. Nanotechnol.* **4** 307–10
[23] Schirmeisen A, Weiner D and Fuchs H 2006 *Phys. Rev. Lett.* **97** 136101
[24] Sugimoto Y *et al* 2008 *Phys. Rev.* B **77** 195424
[25] Chen C J 1993 *Introduction to Scanning Tunneling Microscopy* 1st edn (New York: Oxford University Press)
[26] Pérez R, Štich I, Payne M C and Terakura K 1997 *Phys. Rev. Lett.* **78** 678–81
[27] Pérez R, Payne M C, Štich I and Terakura K 1998 *Phys. Rev.* B **58** 10835–49
[28] Pou P, Ghasemi A, Jelínek P, Lenosky T, Goedecker S and Pérez R 2009 *Nanotechnology* **20** 264015
[29] Enevoldsen G H *et al* 2008 *Phys. Rev.* B **78** 045416
[30] Pinto H P *et al* 2009 *Nanotechnology* **20** 264020

[31] Huang M, Čuma M and Liu F 2003 *Phys. Rev. Lett.* **90** 256101
[32] Zotti L A, Hofer W A and Giessibl F J 2006 *Chem. Phys. Lett.* **420** 177–82
[33] Hug H J *et al* 2001 *Science* **291** 2509a
[34] Lewis J P, Glaesemann K R, Voth G A, Fritsch J, Demkov A A, Ortega J and Sankey O F 2001 *Phys. Rev.* B **64** 195103
[35] Jelínek P, Wang H, Lewis J P, Sankey O F and Ortega J 2005 *Phys. Rev.* B **71** 235101
[36] Kohn W and Sham L J 1965 *Phys. Rev.* **140** A1133–8
[37] Basanta M A, Dappe Y J, Jelínek P and Ortega J 2007 *Comput. Mater. Sci.* **39** 759–66
[38] Ceperley D M and Alder B J 1980 *Phys. Rev. Lett.* **45** 566–9
[39] Oyabu N *et al* 2006 *Phys. Rev. Lett.* **96** 106101
[40] Sugimoto Y *et al* 2006 *Phys. Rev.* B **73** 205329
[41] Lanz M A *et al* 2003 *Phys. Rev.* B **68** 035324
[42] Custance O 2009 private communication